Received: 28 December 2020 | Revised: 16 February 2021 | Accepted: 3 March 2021

DOI: 10.1002/psp4.12620

ARTICLE

A whole-body circulatory neutrophil model with application to predicting clinical neutropenia from *in vitro* studies

Wenbo Chen[1] | **Britton Boras**[2] | **Tae Sung**[2] | **Wenyue Hu**[2] | **Mary E. Spilker**[2] | **David Z. D'Argenio**[1]

[1]Department of Biomedical Engineering, University of Southern California, Los Angeles, California, USA

[2]Pfizer Worldwide Research, Development and Medicine, San Diego, California, USA

Correspondence
David Z. D'Argenio, Department of Biomedical Engineering, University of Southern California, Los Angeles, CA 90089, USA.
Email: dargenio@usc.edu

Funding information
This work was supported by grants from National Institutes of Health/National Institute of Biomedical Imaging and Bioengineering (NIH/NIBIB) P41-EB001978 and the Alfred E. Mann Institute at USC (DZD).

Abstract

A circulatory model of granulopoiesis and its regulation is presented that includes neutrophil trafficking in the lungs, liver, spleen, bone marrow, lymph nodes, and blood. In each organ, neutrophils undergo transendothelial migration from vascular to interstitial space, clearance due to apoptosis, and recycling via the lymphatic flow. The model includes cell cycling of progenitor cells in the bone marrow, granulocyte colony-stimulating factor (G-CSF) kinetics and its neutrophil regulatory action, as well as neutrophil margination in the blood. From previously reported studies, ^{111}In-labeled neutrophil kinetic data in the blood and sampled organs were used to estimate the organ trafficking parameters in the model. The model was further developed and evaluated using absolute neutrophil count (ANC), band cell, and segmented neutrophil time course data from healthy volunteers following four dose levels of pegfilgrastim ($r^2 = 0.77$–0.99), along with ANC time course responses following filgrastim ($r^2 = 0.96$). The baseline values of various cell types in bone marrow and blood, as well as G-CSF concentration in the blood, predicted by the model are consistent with available literature reports. After incorporating the mechanism of action of both paclitaxel and carboplatin, as determined from an *in vitro* bone marrow studies, the model reliably predicted the observed ANC time course following paclitaxel plus carboplatin observed in a phase I trial of 46 patients ($r^2 = 0.70$). The circulatory neutrophil model may provide a mechanistic framework for predicting multi-organ neutrophil homeostasis and dynamics in response to therapeutic agents that target neutrophil dynamics and trafficking in different organs.

Study Highlights

WHAT IS THE CURRENT KNOWLEDGE ON THE TOPIC?

Models for chemotherapy induced neutropenia have been reported and widely applied to characterize the myelosuppressive effects of many different anticancer agents individually and in combination. None of these models, however, reflect our more recent understanding of the roles of organ and tissue heterogeneity in neutrophil trafficking.

WHAT QUESTION DOES THIS STUDY ADDRESS?

A whole-body model of granulopoiesis and its regulation is presented that incorporates the circulatory disposition of neutrophils together with organ-specific transport in the liver, spleen, lung, and bone marrow. The bone marrow subsystem includes a cell cycle model of progenitor cells, which allows for a mechanistic representation of the action of relevant anticancer drugs derived from *in vitro* bone marrow toxicity studies, thereby providing a model-based framework for predicting drug-induced neutropenia from preclinical studies.

WHAT DOES THIS STUDY ADD TO OUR KNOWLEDGE?

The model together with *in vitro* studies of a drug's bone marrow toxicity can predict the extent of neutropenia observed clinically, as illustrated in the case of paclitaxel and carboplatin combinations therapy. The role of neutrophil transendothelial migration and elimination in different tissues, including bone marrow, can be quantified using the model.

HOW MIGHT THIS CHANGE DRUG DISCOVERY, DEVELOPMENT, AND/OR THERAPEUTICS?

Because the model includes neutrophil trafficking and circulation in various tissues, as well as bone marrow granulopoiesis and blood neutrophil mobilization, it provides a mechanistic platform for incorporating the action of different therapeutic agents targeting the above processes.

INTRODUCTION

Neutrophils are central to the innate immune system's response to invading pathogens[1] and also in the pathogenesis of inflammatory diseases of the lung, liver, and kidney.[1–3] Work in recent years has allowed an expanded understanding of the importance of organ-specific differences in migration, activation, and survival of neutrophil granulocytes in infection and inflammatory diseases.[4] Many anticancer therapies disrupt neutrophil homeostasis through their myelosuppressive actions, and whereas a number of models for chemotherapy-induced neutropenia have been developed and applied to many different anticancer agents individually and in combination,[5] none have incorporated the more recent understanding of the roles of organ and tissue heterogeneity in neutrophil trafficking.

Neutrophils are cleared primarily by reticuloendothelial systems in the liver, spleen, lung, and bone marrow.[1] The classical neutrophil recruitment cascade does not operate uniformly in these organs and depends predominantly on the local microvasculature, locally restricted expression of adhesion molecules, as well as interactions with endothelium.[4] Typically, neutrophils are recruited to organs through sequential steps of attachment, rolling, arrest, adhesion, crawling, and transmigration.[4] Upon reaching their eventual transendothelial migration sites, neutrophils cross the endothelial barrier via paracellular or transcellular pathways.[4] Once within the local interstitial space of each organ, neutrophils begin apoptosis and are later removed by macrophages, or initiate phagocytosis-induced cell death, and are subsequently phagocytosed by macrophages.[6] Neutrophils are also recycled via the lymphatic circulation. This local neutrophil processing can vary in different organs and is also altered in infection and chronic inflammatory diseases.[4,6]

The work reported herein presents a model of granulopoiesis and its regulation that incorporates the circulatory disposition of neutrophils together with organ-specific transport and processing. The bone marrow subsystem in the whole-body circulatory model follows our previous model of anticancer drug-induced neutropenia,[7] and includes the cell cycle proliferation of bone marrow progenitor cells. Previously reported kinetic studies with ^{111}Indium (^{111}In)-labeled neutrophils were used to model the neutrophil trafficking in organs (transendothelial migration and elimination), whereas prior pharmacokinetic/pharmacodynamic (PK/PD) studies of pegfilgrastim and filgrastim allowed for the granulocyte colony-stimulating factor (G-CSF) regulatory mechanisms to be incorporated in the model. In this report, the resulting whole-body circulatory model is applied to predict the neutrophil response to combined treatment with paclitaxel and carboplatin observed in a phase I clinical trial.

METHODS

Study data

Radio-labeled neutrophil kinetics

Data from three previously reported tracer kinetic studies of granulocyte disposition in normal humans[8–10] were used

to model the neutrophil trafficking in organs. In these studies, granulocytes were isolated from whole blood, labeled with radioactive ^{111}In, and re-injected to the subjects. Serial blood samples were obtained between 5 min and 48 h following administration of labeled cells. In addition, these studies used dynamic and static gamma camera imaging to record activity in the lung (chest), liver, spleen, and bone marrow (sacro-iliac joints and lumbar spine).[8–10] Reported data were digitized and used in model development as described below. The percent of labeled granulocytes in blood at 13 times over 48 h postinjection were obtained from Figure 1 (normal subjects).[9] The labeled granulocytes in the lungs, liver, spleen, and bone marrow obtained from imaging analysis at various times postinjection were obtained from the references as follows: Figure 4,[8] Figure 4,[9] and Table 2.[10]

Pegfilgrastim, filgrastim PK/PD

Model development also used pegfilgrastim serum concentrations and absolute neutrophil count (ANC), as well as band cell and segmented neutrophil counts following a single s.c. dose of 30 μg/kg, 60 μg/kg, 100 μg/kg, and 300 μg/kg pegfilgrastim obtained from 32 healthy subjects.[11] In addition, mean filgrastim serum concentrations and ANC measurements following a 5 μg/kg filgrastim i.v. infusion and a 1 μg/kg s.c. injection from 24 healthy subjects[12] were used.

In vitro bone marrow toxicity (BMT) assay

As detailed previously,[13] primary human bone marrow mononuclear cells were treated with DMSO, paclitaxel (9

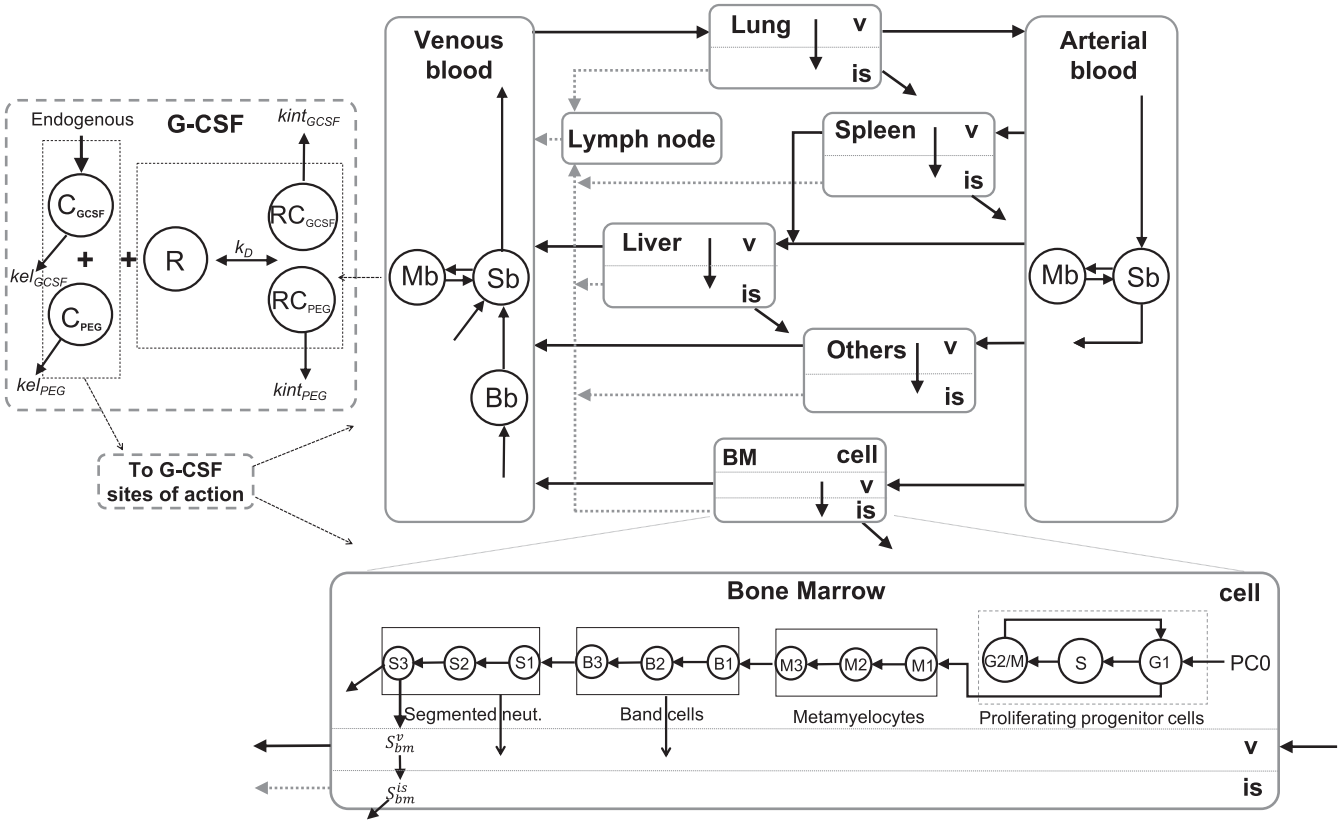

FIGURE 1 Diagram of the circulatory neutrophil model. Bone marrow (BM) granulopoieses includes progenitor cell production (PC0), the proliferating progenitor cell cycle (G1, S, and G2/M), metamyelocytes (Mi), band cells (Bi), and segmented neutrophils (Si). Mature segmented neutrophils (S3) are released to the vascular space (v) and transported to the central venous pool (Sb), or undergo transendothelial migration to the interstitial space (is) to be either cleared or recycled via the lymphatic flow (dotted arrow). Granulocyte colony-stimulating factor (G-CSF) induced release of all stages of segmented neutrophils (Si) and band cells (Bi) is shown (arrows from cell to vascular space), and subsequent circulation to the venous blood (arrows into Sb and Bb). In the venous and arterial blood pools, circulating segmented neutrophils (Sb) exchange with marginated neutrophils (Mb). For other tissues (lung, spleen, liver, and others), neutrophils enter the local vascular space and can undergo transendothelial migration to the organ interstitial space, where they are cleared or recycled via the lymphatic system. The dashed box on the left represents G-CSF kinetics and regulatory subsystem. Endogenous production and clearance of G-CSF are included, as is the linear and target-mediated disposition of administered filgrastim and pegfilgrastim. G-CSF's stimulatory effects on proliferation of progenitor cells (PCs) in bone marrow, maturation in bone marrow, and mobilization from bone marrow to blood and on blood margination are indicated by the dashed arrows. The complete set of model equations is provided in the Supplementary Information S1

concentrations from 0.0762 nM to 500 nM), or carboplatin (9 concentrations from 0.00762 μM to 50 μM) for 5 days, at which time cell viability was assessed. The *in vitro* BMT assay results were used to model the action of paclitaxel and carboplatin on the bone marrow progenitor cell cycle (see below).

Clinical trial of paclitaxel and carboplatin combination therapy

Data from a previously conducted phase I clinical trial of paclitaxel plus carboplatin in 46 patients with multiple advanced solid malignancies[14] were used to evaluate model predictions. As described,[14] patients received paclitaxel as a 3 h i.v. infusion on day 0 with doses ranging from 150 mg/m^2 to 200 mg/m^2, followed by a 30 min i.v. infusion of carboplatin targeting an area under the curve of 6 mg·min/ml. Data from this trial included individual subject plasma free carboplatin concentrations and ANC counts on days 0, 7, 14, and 21. Neutropenia grade was classified in each patient according to Common Terminology Criteria for Adverse Events.[15]

Model development, parameter estimation, clinical trial predictions, and simulations

Circulatory model with bone marrow granulopoiesis, blood margination, G-CSF kinetics

The complete circulatory model, including neutrophil disposition and trafficking in organs, granulopoiesis in the bone marrow, neutrophil margination in the blood, G-CSF kinetics, and regulation is shown in Figure 1. The model incorporates those organs that are primarily responsible for neutrophil hemostasis in health and disease[1]: venous and arterial blood, lungs, liver, spleen, lymph node, and bone marrow. A lumped compartment represents remaining tissues including the heart, kidneys, muscle, skin, and gastrointestinal tract. Each organ includes a vascular space with neutrophil transendothelial migration[4] to its interstitial space, where neutrophils are then phagocytosed by macrophages[16] or recycled via the lymphatics.[17] The circulatory model also includes neutrophil margination in the venous and arterial blood pools, as well as G-CSF kinetics (with filgrastim or pegfilgrastim support therapy) and its regulatory action, as described previously.[7] The complete set of equations for the model depicted in Figure 1 is provided in the Supplementary Information S1and S2. Values for circulatory parameters of the model (mean and SD), including blood and lymph flow rates, vascular, and extravascular tissue volumes in various organs, are listed in the Supplementary Information S3 and were taken from refs. 18 and 19

As in our previous model,[7] the bone marrow subsystem includes a cell cycle model of progenitor cells (PCs), which allows for a mechanistic representation of the action of relevant anticancer drugs derived from *in vitro* bone marrow toxicity studies, as illustrated below. The following equations (from the complete model in supplementary Information) describe mature segmented neutrophils in the red bone marrow:

$$\frac{dS3}{dt} = \frac{3}{\tau seg \cdot \left(1 - \frac{Imax^{BM}_{GCSF} \cdot GCSF}{EC50^{BM}_{GCSF} + GCSF}\right)} \cdot S2 - \left(\frac{3}{\tau seg} + \frac{Emax^{seg}_{GCSF} \cdot GCSF}{EC50^{BM}_{GCSF} + GCSF} + k_{ig}\right) \cdot S3 \quad (1)$$

$$\frac{dS^{v}_{bm}}{dt} = \left(\frac{3}{\tau seg} \cdot S3 + \frac{Emax^{seg}_{GCSF} \cdot GCSF}{EC50^{BM}_{GCSF} + GCSF} \cdot (S1 + S2 + S3)\right) \cdot V^{cell}_{bm} / V^{v}_{bm} + (Q_{bm} \cdot Sb_{artery} - (Q_{bm} - L_{bm}) \cdot S^{v}_{bm} - CL^{tm}_{bm} \cdot S^{v}_{bm}) / V^{v}_{bm} \quad (2)$$

$$\frac{dS^{is}_{bm}}{dt} = \frac{\left(CL^{tm}_{bm} \cdot S^{v}_{bm} - L_{bm} \cdot S3^{is}_{bm} - CL^{el}_{bm} \cdot S^{is}_{bm}\right)}{V^{is}_{bm}} \quad (3)$$

where $S1$, $S2$, and $S3$ represent the concentration of segmented neutrophils in each of the three stages of segmented neutrophil maturation, whereas S^{v}_{bm} and S^{v}_{bm} represent neutrophil concentrations in the bone marrow vascular and interstitial spaces. Equation 1 represents the last stage of mature segmented neutrophils, including G-CSF induced mobilization within the cell compartment of bone marrow ($Emax^{seg}_{GCSF}$, $EC50^{BM}_{GCSF}$) and maturation of segmented neutrophils from stage 2 to 3 ($Imax^{BM}_{GCSF}$, $EC50^{BM}_{GCSF}$) with time constant τseg, as well as incomplete granulopoiesis (k_{ig}). Line 1 of Equation 2 represents the release of neutrophils into the local vascular space of bone marrow (first term), and the G-CSF induced mobilization to the vascular space (second term). Line 2 of Equation 2 represents the recirculation of neutrophils through the bone marrow (first 2 terms), as well as transendothelial migration ($CL^{tm}_{bm} \cdot S^{v}_{bm}$). Equation 3 represents neutrophils in interstitial space of bone marrow, which includes the elimination of neutrophils ($CL^{el}_{bm} \cdot S^{is}_{bm}$; see Supplementary Information for complete model equations).

Modeling neutrophil trafficking in organs from tracer studies

Following the trace injection of radio-labeled neutrophils, production and release of neutrophils from bone marrow, their margination in blood, as well as G-CSF levels, were assumed to be unaltered from their basal states. Accordingly, the model equations given in supplementary Information S2

describe the kinetics and organ disposition of labeled neutrophils. These tracer kinetic model equations and the fixed circulatory parameters' values (Supplementary Information S3), together with the pooled labeled neutrophil data in each organ (lung, liver, spleen, bone marrow, and blood) over 48 h, were used to estimate each tissue' transendothelial migration and elimination clearance listed in Table 1. The naïve pooled data (NPD) analysis estimation application in ADAPT (version 5)[20] was used to obtain the maximum likelihood estimates of parameters assuming an additive plus proportional error variance model (model code provided in Data S1 of Supporting Information).

Estimating G-CSF related model parameters from pegfilgrastim, filgrastim PK/PD data

All the pegfilgrastim PK/PD data, including serum concentrations, ANC, band cell, and segmented neutrophil counts following each of the four s.c. doses, along with the filgrastim serum concentrations and ANC values following i.v. and s.c. doses were pooled to obtained the maximum likelihood estimates of the remaining unknown parameters in the circulatory model (NPD application in ADAPT,[20] with separate additive and proportional error variance for each output). The neutrophil transendothelial migration and elimination clearances were fixed at their values estimated from the tracer kinetic analysis. The estimated model parameters included the G-CSF related parameters ($EC50^{PC}_{GCSF}$, $Emax^{PC0}_{GCSF}$, $Emax^{PC-M}_{GCSF}$, $EC50^{BM}_{GCSF}$, $Emax^{band}_{GCSF}$, $Emax^{seg}_{GCSF}$, $Imax^{BM}_{GCSF}$, k_{BS}), rate constant of ineffective granulopoiesis (k_{ig}), the circulating fraction of neutrophils (f_{tissue}), along with parameters defining the kinetics of endogenous G-CSF, filgrastim (k^{GCSF}_{el}, k^{GCSF}_{int}), and pegfilgrastim (k^{PEG}_{el}, k^{PEG}_{int}). The remaining parameters were fixed as previously reported.[7] Table 2 lists the estimated and fixed parameters, and together with the fixed circulatory parameters in Table S1, completely define all model parameters. Because the baseline value of each state in the model depends on the unknown parameter values, a predose period (1000 h) was added to allow the steady-state basal values to be reached.

Model evaluation: Predicting ANC time course and neutropenia grade following paclitaxel plus carboplatin combination therapy

As described previously,[7] the *in vitro* BMT assay results were used to quantify the action of paclitaxel and carboplatin on the progenitor cell cycle. In the bone marrow subsystem in Figure 1, paclitaxel was assumed to induce apoptosis of G2/M-phase cells in the model, whereas carboplatin was assumed to induced apoptosis of PCs in each of the three modeled phases of mitosis (G1, S, and G2/M). The drug action parameters for paclitaxel and for carboplatin were each estimated using the corresponding BMT assay data and the bone marrow subsystem model in Figure 1, as reported in refs. 7 and 13.

Using the complete set of model parameters and available standard deviations, the dose regimens of paclitaxel and carboplatin administered to each of the 46 patients in the above cited clinical trial were used to simulate the model response for each patient ($n = 1000$ simulations for each patient). The simulation application (SIM) in ADAPT (version 5) was used, with model parameters assumed to be independent, lognormally distributed.[20] The resulting ANC-time profiles from the 100 simulations with baseline ANC values closest to each patient's measured baseline ANC were used to calculate the median and prediction interval (PI) of the ANC-time profile for that patient (baseline matched ANC time course). The PI was determined as the largest and smallest ANC values at each time point from the 100 ANC time profiles. The individual patient-predicted baseline matched median ANC time profile, PI, and neutropenia grade (determined from the median ANC profile) were compared with observed ANC values and neutropenia grade in each patient.

TABLE 1 Model parameter estimates obtained from radiolabeled neutrophil studies

Parameter (unit)	Definition	Estimate (RSE%)
CL^{tm}_{lung}(L/h)	Transendothelial migration clearance in lung	2.63 (10)
CL^{tm}_{liver}(L/h)	Transendothelial migration clearance in liver	1.15 (11)
CL^{tm}_{spleen}(L/h)	Transendothelial migration clearance in spleen	3.59 (11)
CL^{tm}_{bm}(L/h)	Transendothelial migration clearance in bone marrow	0.753 (7.3)
CL^{el}_{lung}(L/h)	Neutrophil elimination clearance in lung	0.36 (28)
CL^{el}_{liver}(L/h)	Neutrophil elimination clearance in liver	0.195 (6.6)
CL^{el}_{spleen}(L/h)	Neutrophil elimination clearance in spleen	0.0169 (15)
CL^{el}_{bm}(L/h)	Neutrophil elimination clearance in bone marrow	0.0672 (11)

TABLE 2 Model parameter estimates obtained from pegfilgrastim and filgrastim studies

Parameter (unit)	Definition	Estimate (RSE%)
$EC50^{PC}_{GCSF}$ (ng/ml)	Concentration of G-CSF eliciting a half-maximal effect on progenitor cells	4.10 (13)
$Emax^{PC0}_{GCSF}$ (−)[a]	Relative maximum G-CSF-stimulated production of progenitor cells	3.34 (−)
$Emax^{PC-M}_{GCSF}$ (−)	Relative maximum G-CSF-stimulated differentiation to metamyelocyte	1.17 (8.0)
$Imax^{BM}_{GCSF}$ (−)	Maximum G-CSF-inhibition of mean maturation times	0.494 (6.5)
$EC50^{BM}_{GCSF}$ (ng/ml)	Concentration of G-CSF eliciting a half-maximal effect on all maturation times and on mobilization of bone marrow cells	2.87 (5.2)
$Emax^{band}_{GCSF}$ (1/h)	Rate constant for maximum G-CSF-stimulated mobilization of bone marrow band cells into blood	0.00421 (2.5)
$Emax^{seg}_{GCSF}$(1/h)	Rate constant for maximum G-CSF-stimulated mobilization of bone marrow segmented neutrophils into blood	0.0343 (2.9)
k_{ig} (1/h)	Rate constant for ineffective granulopoiesis from bone marrow	0.103 (6.5)
k_{BS} (1/h)	Rate constant for maturation of band cells in blood to segmented neutrophils	0.0653 (4.2)
f_{tissue} (−)	Fraction of neutrophils circulate to tissue from blood	0.226 (14)
k^{GCSF}_{el} (1/h)	G-CSF elimination rate constant	0.374 (2.0)
k^{GCSF}_{int} (1/h)	Receptor-mediated G-CSF internalization rate constant	0.0807 (27)
k^{PEG}_{el} (1/h)	Pegfilgrastim elimination rate constant	0.02533 (4.0)
k^{PEG}_{int} (1/h)	Receptor-mediated pegfilgrastim internalization constant	1.55 (1.3)

The remaining parameters were fixed as reported previously[7] and are listed in the Supplementary Information S3.

Abbreviation: G-CSF, granulocyte colony-stimulating factor.

[a]Secondary parameter: $Emax^{PC0}_{GCSF} = 2 \cdot Emax^{PC-M}_{GCSF}$.

Simulating the effects of organ neutrophil transendothelial migration and elimination on tissue neutrophil trafficking and ANC

The model was used to provide insights into the distribution of neutrophils among tissues, secondary to changes in organ neutrophil transendothelial migration and elimination. The clearances for neutrophil transendothelial migration and elimination in the lung, liver, spleen, and bone marrow were independently changed to 0.1, 0.5, 2, and 10 times their original values (25 pairs of these 2 neutrophil trafficking parameters in each tissue). Total neutrophil counts in the respective tissues (vascular plus interstitial), along with the corresponding ANC counts, were recorded and compared to the baseline values. The ANC changes were expressed as a percent change from baseline value, while fold changes from baseline were recorded for the lung, liver, spleen, and bone marrow.

RESULTS

Radio-labeled neutrophil kinetics in organs

The estimation results from the ^{111}In-labeled neutrophil data and the tracer kinetic circulatory model are given in Table 1 and Figure 2a. The organ transendothelial migration clearances were estimated with good precision (RSE% ranging from 7.3% to 11%), except for CL^{tm}_{other} and this pathway was not included in the final model (a single pool was used to represent "other" tissues). The corresponding time constants ranged from 0.2 min to 8.3 min and are consistent with those obtained from in vitro studies of neutrophil transendothelial mobilization, the majority of which are between 1 and 10 min.[21] The estimated tissue neutrophil clearances (Table 1) varied over a 20-fold range, from 0.0169 L/h in the spleen to 0.36 L/h in the lungs (RSE% ranging from 6.6% to 28%), with time constants range from 35 min to 173 min.

Pegfilgrastim and filgrastim in healthy volunteers

Table 2 and Figure 2b,c show the estimation results from the circulatory model in Figure 1 obtained using the pooled pegfilgrastim and filgrastim data. The model captures the dose-dependent, multiphasic behavior of pegfilgrastim PK concentration, along with ANC, band cell, and segmented neutrophil time course (Figure 2b), and simultaneously describes the PK and ANC response to both s.c. and i.v. administration of filgrastim (Figure 2c). The parameters in Table 2 were reliably estimated with acceptable standard errors (RSE% < 30%), which are the consequences of the rich information provided in the pooled pegfilgrastim and filgrastim data. The majority of the estimated parameter values in Table 2 are comparable to the values in our previously reported model[7] (within a factor of 2 or less), with the exception of $EC50^{PC}_{GCSF}$. Nonetheless, the estimated value of 4.1 ng/

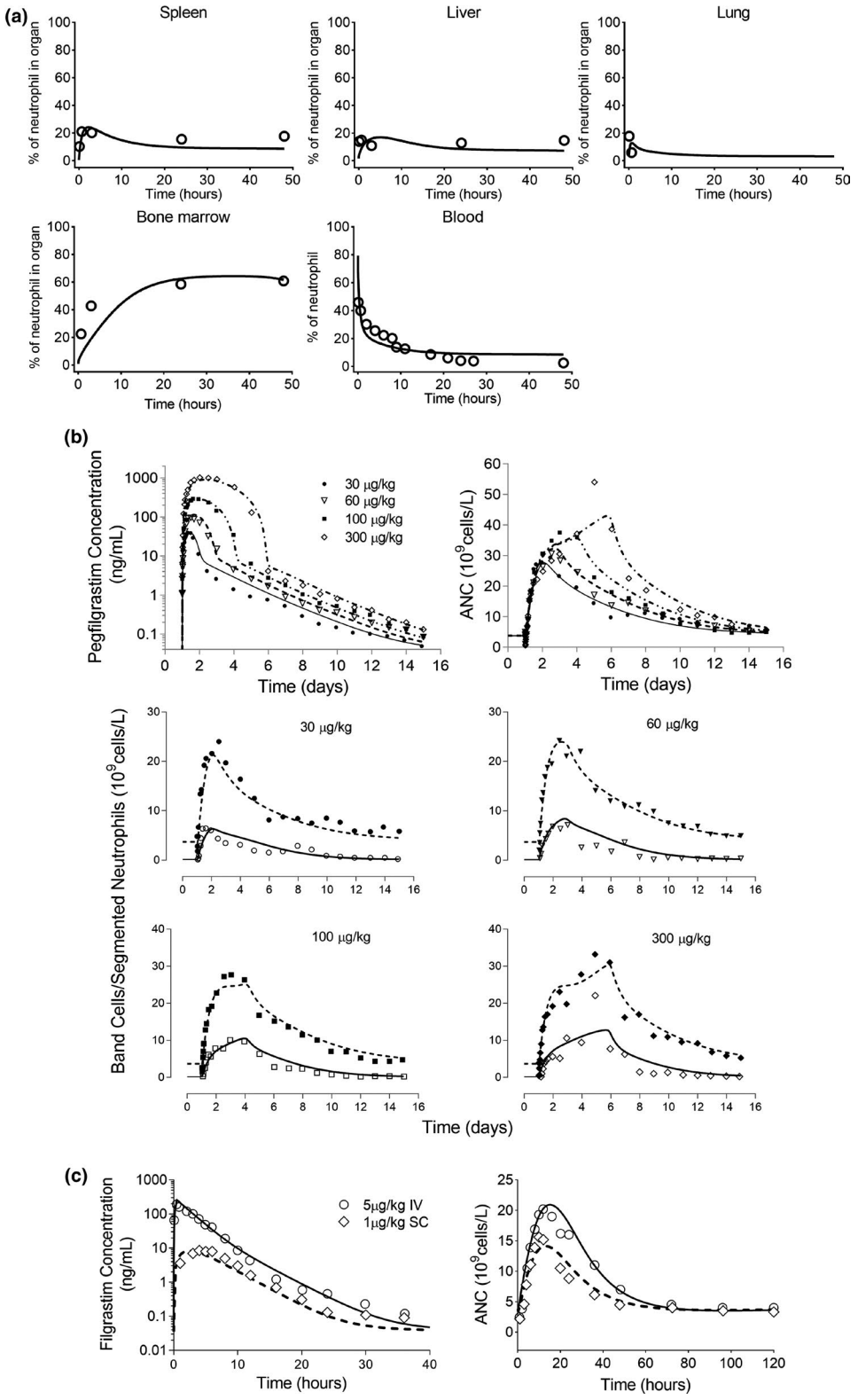

FIGURE 2 (a) Tracer studies: model predicted (lines) and observed (symbols) radiolabeled neutrophil kinetics in the spleen, liver, lung, bone marrow, and blood. Overall observed versus predicted r^2 values: spleen = 0.74, liver = 0.57, lung = 0.80, bone marrow (BM) = 0.90, and blood = 0.80. (b) Pegfilgrastim: the six graphs show model predicted (lines) and observed (symbols) pegfilgrastim concentration, absolute neutrophil count (ANC), band cells (solid lines), segmented neutrophils (dashed lines) following 30, 60, 100, and 300 μg/kg s.c. of pegfilgrastim. Overall observed versus predicted r^2 values: pegfilgrastim concentration = 0.99, ANC = 0.95, band cells = 0.77, and segmented neutrophils = 0.94. (c) Filgrastim: the two graphs show model predicted (lines) and observed (symbols) filgrastim concentration and ANC following i.v. (5 μg/kg) and s.c. (1 μg/kg) of filgrastim. Overall observed versus predicted r^2 values: filgrastim concentration = 0.92 and ANC = 0.96

ml lies between the reported overall half-maximal effective concentration (EC_{50}) of pegfilgrastim (9.86 ng/ml)[11] and filgrastim (3.15 ng/ml).[12]

Model-predicted basal physiological values

The circulatory model was simulated to predict the distribution of basal values of all model states in adult humans using parameter values and from Tables 1 and 2, along with the circulatory system parameter values (see Table S3 for complete set of model parameter values). As shown in Figure 3, the model-predicted distributions of the different cell types in the bone marrow (PC, metamyelocyte, band cell, and segmented neutrophil) are consistent with their reported ranges in healthy subjects.[22] The distribution of the simulated values of the basal pool sizes of ANC, blood band cells, segmented and marginated neutrophils, as well as blood G-CSF concentration are also consistent with literature reported values, as shown in Figure 3. The model-predicted median and mean values of ANC are 4.2×10^9 and 5×10^9 cells/L, which are comparable to the range of typical mean and median values of ANC ($4.2–4.7 \times 10^9$ cells/L) reported in healthy subjects.[23] Approximately 80% of the simulated ANC values lie within the normal range for healthy adults ($1.5–8.0 \times 10^9$ cells/L), whereas 6% of the simulated ANC values are below 1.5×10^9 cells/L, which is also consistent with other reports.[23] The model-predicted median value of marginated neutrophils is 4.7×10^9 cells/L, resulting in a marginated to circulating neutrophil ratio of 1.1, within the range reported for healthy adults (0.23–4.9).[24] The model-predicted median G-CSF concentration (0.03 ng/ml) is also within the normal range for adults (<0.03–0.163 ng/ml).[25]

Predicting paclitaxel plus carboplatin-induced neutropenia

The top panel of Figure 4 shows the model-predicted ANC time course profiles (median and PI) of selected trial

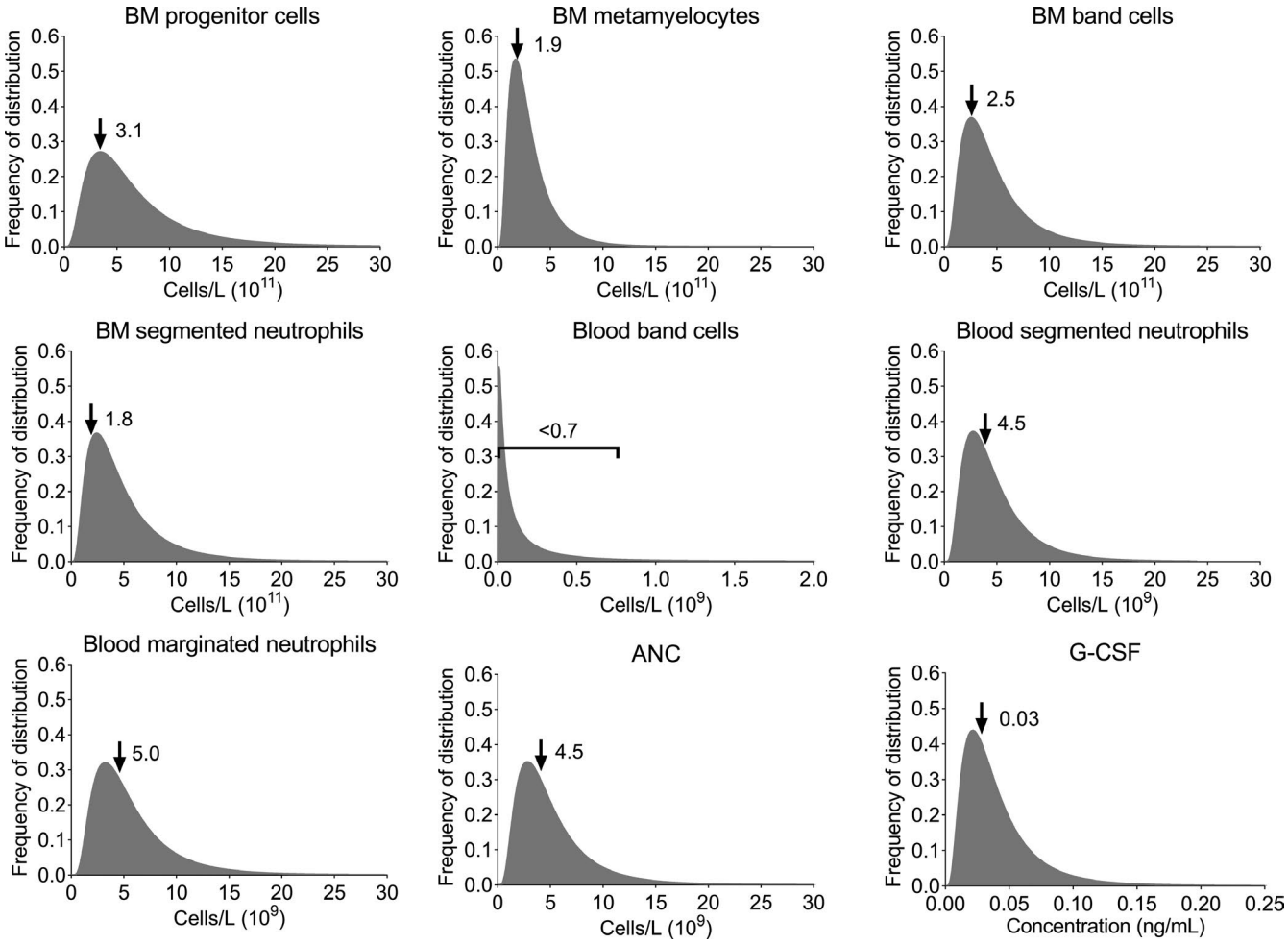

FIGURE 3 Model-simulated distribution of basal values for each cell type in bond marrow (BM) and blood, as well as granulocyte colony-stimulating factor (G-CSF) concentration in the blood. Shaded area: distribution from the 1000 subjects. Arrows: literature reported value. ANC, absolute neutrophil count

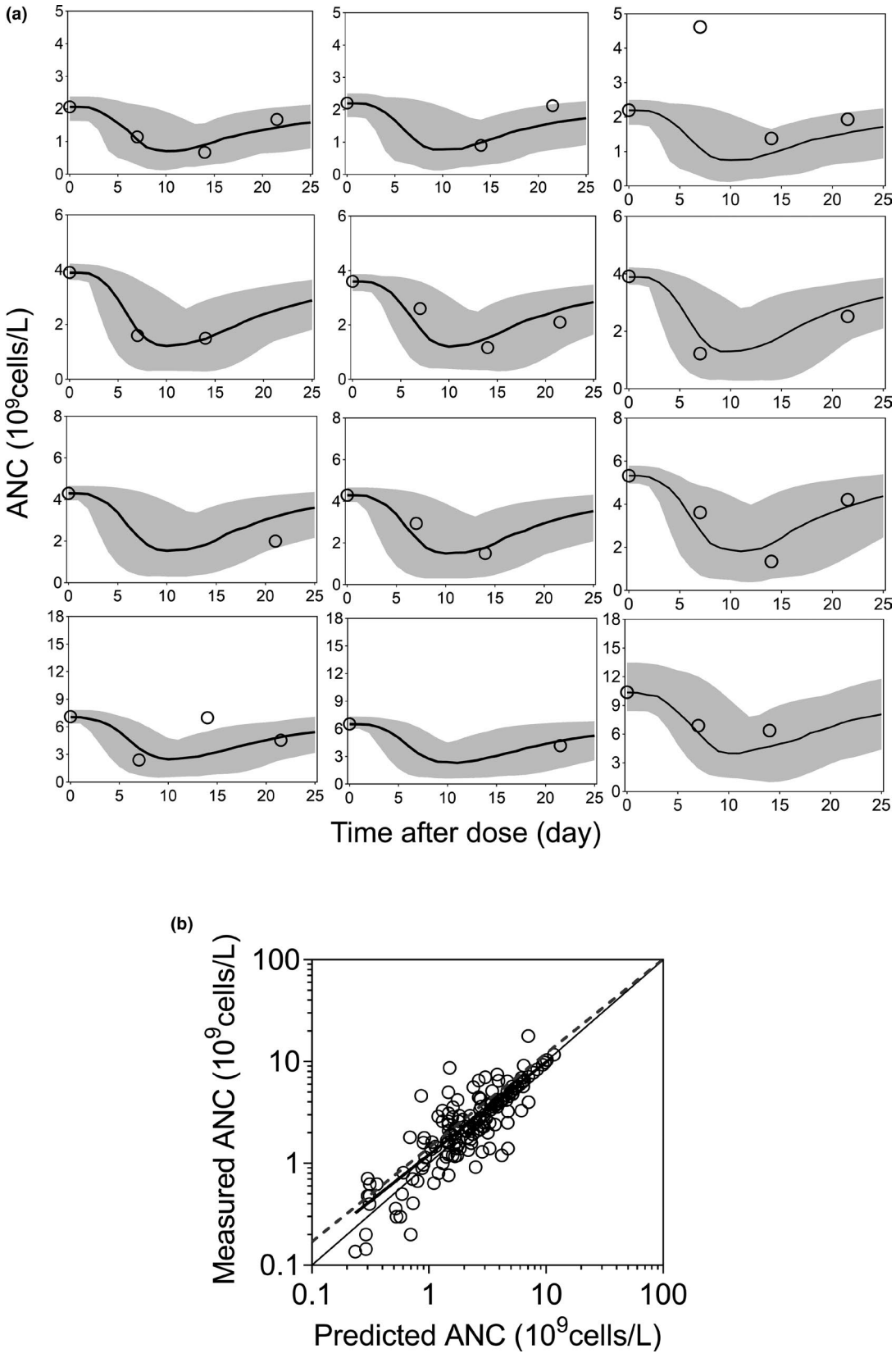

FIGURE 4 Model predictions versus observations from a phase I clinical trial of paclitaxel plus carboplatin combination therapy. Top panels: Model predicted (line = median; shaded area = prediction interval) and measured (symbols) absolute neutrophil count (ANC) time profiles in 12 representative patients from four baseline ANC (BANC) groups (3 per group), with BANC ranges less than 3.3 $\times 10^9$ (first row), between 3.3 and 4.2 $\times 10^9$ (second row), between 4.2 and 5.9 $\times 10^9$ (third row), and above 5.9 $\times 10^9$ cells/L (fourth row). Bottom graph: Model predicted versus measured ANC values in all patients. Symbols = measurements; solid line = line of identity; dashed line = regression line

patients in four different baseline ANC ranges: ANC less than 3.3×10^9 (first row), between 3.3 and 4.2×10^9 (second row), between 4.2 and 5.9×10^9 (third row), and greater than 5.9×10^9 cells/L (fourth row). Predicted ANC values in all patients correlate with measured ANC ($r^2 = 0.70$) and are distributed symmetrically around the line of identity with a slope of 0.91 (Figure 4 bottom panel). Model simulation using the median dose used in the trial patients predicted that ~ 41% of patients develop grade 3 or 4 neutropenia, which is similar to the observation of 39% of patients from the trial. The observed versus model-predicted incidences of grades 2, 3, and 4 neutropenia are, respectively, 23.9% versus 22.4%, 17.3% versus 30.3%, and 21.7% versus 10.2%, indicating the limitation of the model to distinguish grades 3 and 4 neutropenia in the example.

Simulating response to changes in tissue neutrophil transendothelial migration and elimination

Figure 5 presents the results of changing both neutrophil transendothelial migration and elimination clearances in the lung (top left), liver (top right), and spleen (lower left) for that tissue, with neutrophil counts in each tissue increasing with increasing transendothelial migration clearance and

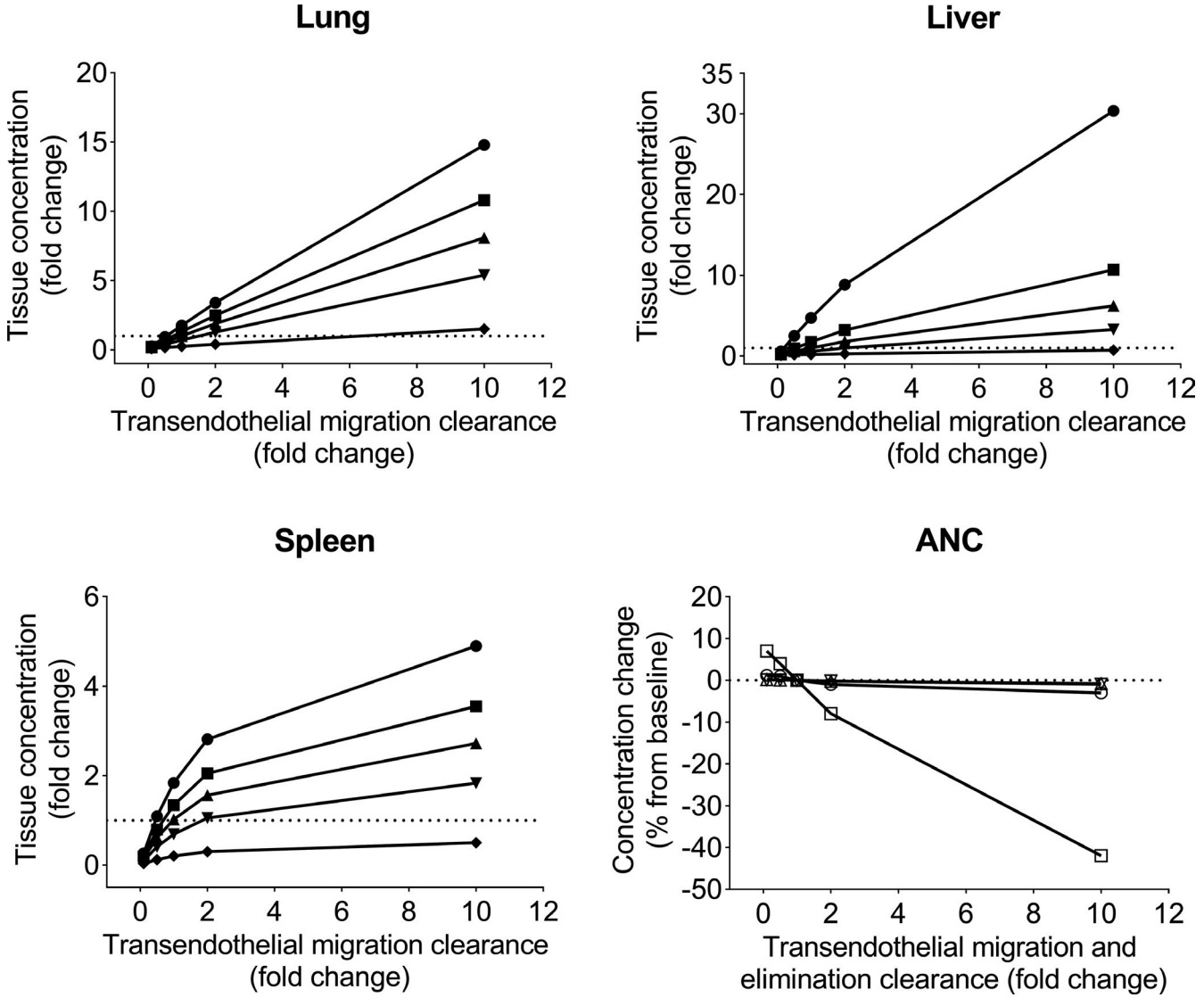

FIGURE 5 Model predicted effects of tissue parameter changes on absolute neutrophil count (ANC) and organ neutrophil counts. Solid lines with symbols—simulation results, horizontal dotted lines—basal values using the nominal parameter values (Table 1). For the lung (top left), liver (top right), and spleen (bottom left): filled circle = 0.1-fold change in elimination clearance in the respective organ; filled square = 0.5-fold change; filled triangle = 1-fold change; filled inverted triangle = 2-fold change; and filled diamond = 10 fold change. For the ANC plot on the bottom right: open circle = lung; open triangle = spleen; open inverted triangle = liver; and open square = bone marrow

decreasing elimination clearance. Changing these parameters in bone marrow had little effect on cell counts in bone marrow due to the large pools of cells from granulopoiesis (figure not shown). Although the lung and liver showed a mostly linear relation between tissue cell counts and transendothelial migration clearance at their nominal elimination clearances (lines denoted by ▲), for the spleen this relationship was nonlinear. The bottom right panel of Figure 5 shows the extent of changes in ANC resulting from simultaneous increases and decreases in transendothelial migration and elimination clearances from their nominal values in each tissue. These changes in the tissue parameters in the lung, liver, and spleen had little effect on ANC, even though they have significant effects on the respective organ neutrophil levels, reflecting autoregulatory action of the system to maintain homeostasis. In bone marrow, while decreasing the bone marrow trafficking clearances produced only modest increases in ANC, increasing these clearances overwhelms the autoregulatory capability of the system to maintain homeostasis, resulting in significant neutropenia. Sensitivity of ANC to other model parameters has been reported previously.[7]

DISCUSSION

A whole-body circulatory model of granulopoiesis and its regulation is presented to predict neutrophil counts in blood, bone marrow, lung, spleen, liver, and lymph node. The model was used to characterize the ^{111}In-labeled neutrophil kinetics in selected organs in healthy humans, thus allowing estimation of neutrophil migration and elimination clearances in individual tissues, and the effects of pegfilgrastim and filgrastim-induced neutrophilia observed in humans. Model predictions of basal levels of the different cell types in the bone marrow and blood were consistent with available measured values, as reported in the literature. The circulatory model also adequately predicted the neutrophil response observed in patients treated with paclitaxel plus carboplatin in a phase I clinical trial, based solely on results from *in vitro* bone marrow toxicity studies.

Combining results from several tracer kinetic *ex vivo* ^{111}In-labeled neutrophil studies[8–10] provided a basis for estimating the neutrophil transendothelial migration and elimination rate constants in the liver, spleen, lung, and bone marrow, as shown in Table 1 and Figure 2. Other commonly used neutrophil labeling techniques, include diisopropylfluorophosphate (DF^{32}P), ^{3}H-TdR, ^{51}Cr, and technetium-99 m (^{99m}Tc),[26] have also been validated across species and have all resulted in similar estimates of blood neutrophil half-life in the range of 5–8 h.[22,26] While these labeling techniques have different advantages and limitations, ^{111}In demonstrates specific labeling upon cell separation, high labeling efficiency, rapid excretion after cell death, and no interference with cell traffic.[26–28] As with each of these different lymphocyte labeling techniques,[29] it is expected that the different neutrophil labeling techniques may also result in differences in observed organ kinetic profiles at the later times. However, given the relative short 2-day period of the tracer results used in this work, the problems associated with longer term labeling experiments are minimized. We note also that the model can be used to incorporate the results from studies using newer *in vivo* labeling technologies as they become available,[22] which may result in a better assessment of the tissue neutrophil time course profile than used in the current study.

The previously reported[11] blood neutrophil time course responses following pegfilgrastim (ANC, band cell, and segmented neutrophil) and filgrastim (ANC) administration used in this work, resulted in a wide range of G-CSF exposures (in magnitude and time course) that allowed reliable estimation of the G-CSF related parameters in the circulatory model. In contrast, if only neutrophil responses secondary to administration of myelosuppressive agents were used, it would have limited the ability to estimate the different G-CSF related parameters (bone marrow and margination) in the circulatory model, given the closed-loop nature of the neutrophil-G-CSF system.[30]

The circulatory model predicted median and mean values, as well as ranges of ANCs, that are consistent with the values in normal adults (Figure 3). We note that the data used to develop the model and predict the results in Figure 3 were obtained from healthy humans. While the predicted basal values of bone marrow cell types, blood band cells, segmented and marginated neutrophils are also similar to measured values reported in the literature, these are based on measurements in a very small number of subjects—unlike ANC. While organ transit times can be calculated from the model (lung = 2.3 min, liver = 9.4 min, spleen = 0.3 min, and bone marrow = 12 min), these predictions cannot be evaluated due to lack of reliable experimental measurements.

In this report, the circulatory model was applied to predict the neutrophil response to paclitaxel plus carboplatin treatment in 46 patients from the control arm of a recent phase I trial,[14] following the framework that we applied previously using a non-circulatory model of anticancer drug-induced neutropenia.[7,13] As shown in Figure 4, the circulatory model incorporating the mechanisms of action of paclitaxel and carboplatin (as determined from *in vitro* studies), satisfactorily predicted the ANC time course in the clinical trial patients over a wide range of baseline ANC values, and provides a basis for further evaluating the model's predictive ability with other anticancer agents. The model can also be used to explore dosing strategies for G-CSF therapies to support neutrophil homeostasis in patients undergoing anticancer drug treatment, for example, to assess the effects of filgrastim and pegfilgrastim following treatment with paclitaxel and carboplatin.[13] Beyond anticancer agents, drug-induced neutropenia

is associated with many other drug classes that induce myelosuppression, accelerate neutrophil apoptosis and elimination, or alter neutrophil margination and migration.[31] For example: (1) anti-TNF-α therapy sensitizes neutrophils, leading to their immune-mediated peripheral destruction; (2) rituximab may favor B-cell repopulation and impair granulopoiesis; (3) tocilizumab-induced neutropenia is attributed to accelerate neutrophil apoptosis and intravascular margination; and (4) alemtuzumab-related late onset neutropenia, which may be due to autoimmune neutropenia mechanisms, can be treated with G-CSF.[32] Accordingly, the circulatory model-based framework presented in this work is applicable to a range of other therapies that result in neutropenia, as part of an effort to investigate *in vitro* to clinical translation during early drug development.

The model also provides insights into the role of organ-specific transendothelial migration and elimination on neutrophil homeostasis as shown in Results, as well as the effects of altered margination (results not shown). The proposed circulatory model, therefore, has application to better understanding the actions of therapies that reduce neutrophil adhesion to endothelial cells and subsequent transendothelial migration, or alter neutrophil phenotype and thus elimination clearance.[33] Some examples for potential model application include: (1) nanomedicine drug carriers modified with antibodies and ligands that selectively bind to overexpressed endothelial cellular adhesion molecules in inflammation, thus reducing neutrophil adhesion[33]; (2) selectin-blocking agents that inhibit CXCL1 and ICAM1, leading to a reduction in hepatic neutrophil infiltration, which may ameliorate liver injury[3]; (3) the inhibition of interleukin-6 receptor by sarilumab and tocilizumab that induces margination and therefore alters ANC[34,35]; and (4) targeting molecular pathways within neutrophils that lead to the formation of reactive oxygen species and neutrophil extracellular traps, both of which mediate neutrophil apoptosis.[3]

In contrast to other reported models of drug-induced neutropenia, the model presented in this report incorporates the circulatory disposition of neutrophils, together with organ-specific neutrophil transport and processing in the lung, spleen, liver, as well as bone marrow, while also including the cell cycle proliferation of bone marrow progenitor cells. Because the model includes subsystems representing bone marrow granulopoiesis, blood neutrophil mobilization, neutrophil trafficking and circulation in various tissues, as well as regulation via G-CSF, it provides a mechanistic platform for incorporating the action of therapeutic agents targeting the above processes. Moreover, as illustrated with carboplatin/paclitaxel therapy, the model can predict clinical neutropenia of compounds under development based solely on *in vitro* bone marrow studies.

ACKNOWLEDGEMENTS

The authors gratefully acknowledge Dr. Jan H. Beumer from the Cancer Therapeutics Program, and the Departments of Pharmaceutical Sciences and Medicine at the University of Pittsburgh for providing the paclitaxel/carboplatin clinical trial data.

CONFLICT OF INTEREST

W.C. and D.Z.D. declare no conflict of interests. B.B., T.S., W.H., and M.E.S. are employees of Pfizer, Inc. These authors have no other relevant affiliations or financial involvement with any organization or entity with a financial interest in or financial conflict with the subject matter or materials discussed in the manuscript apart from those disclosed.

AUTHOR CONTRIBUTIONS

W.C. and D.Z.D. wrote the manuscript. W.C., D.Z.D., B.B., and M.E.S. designed the research. W.C. and D.Z.D. performed the research. T.S. and W.H. contributed new reagents/analytical tools.

REFERENCES

1. Hidalgo A, Chilvers ER, Summers C, Koenderman L. The neutrophil life cycle. *Trends Immunol*. 2019;40:584-597.
2. Silvestre-Roig C, Hidalgo A, Soehnlein O. Neutrophil heterogeneity: implications for homeostasis and pathogenesis. *Blood*. 2016;127:2173-2181.
3. Bartneck M, Wang J. Therapeutic targeting of neutrophil granulocytes in inflammatory liver disease. *Front Immunol*. 2019;10:1-18.
4. Maas SL, Soehnlein O, Viola JR. Organ-specific mechanisms of transendothelial neutrophil migration in the lung, liver, kidney, and aorta. *Front Immunol* 2018;9:2739.
5. Schirm S, Engel C, Loeffler M, Scholz M. Modelling chemotherapy effects on granulopoiesis. *BMC Syst Biol*. 2014;8:138.
6. Kobayashi SD, Malachowa N, DeLeo FR. Influence of microbes on neutrophil life and death. *Front Cell Infect Microbiol*. 2017;7:159.
7. Chen W, Boras B, Sung T, et al. A physiological model of granulopoiesis to predict clinical drug induced neutropenia from in vitro bone marrow studies: with application to a cell cycle inhibitor. *J Pharmacokinet Pharmacodyn*. 2020;47:163-182.
8. Peters AM, Saverymuttu SH, Bell RN, Lavender JP. Quantification of the distribution of the marginating granulocyte pool in man. *Scand J Haematol*. 1985;34:111-120.
9. Saverymuttu SH, Peters AM, Keshavarzian A, Reavy HJ, Lavender JP. The kinetics of 111Indium distribution following injection of 111Indium labelled autologous granulocytes in man. *Br J Haematol*. 1985;61:675-685.
10. Szczepura KR, Ruparelia P, Solanki CK, et al. Measuring whole-body neutrophil redistribution using a dedicated whole-body counter and ultra-low doses of 111Indium. *Eur J Clin Invest*. 2011;41:77-83.
11. Roskos LK, Lum P, Lockbaum P, Schwab G, Yang BB. Pharmacokinetic/pharmacodynamic modeling of pegfilgrastim in healthy subjects. *J Clin Pharmacol*. 2006;46:747-757.
12. Krzyzanski W, Wiczling P, Lowe P, et al. Population modeling of filgrastim PK-PD in healthy adults following

intravenous and subcutaneous administrations. *J Clin Pharmacol*. 2010;50:101S-112S.
13. Chen W, Boras B, Sung T, Hu W, Spilker ME, D'Argenio DZ. Predicting chemotherapy-induced neutropenia and granulocyte-colony stimulating factor response using model-based in vitro to clinical translation. *AAPS J*. 2020;22(6):143.
14. Appleman LJ, Beumer JH, Jiang Y, et al. Phase 1 study of veliparib (ABT-888), a poly (ADP-ribose) polymerase inhibitor, with carboplatin and paclitaxel in advanced solid malignancies. *Cancer Chemother Pharmacol*. 2019;84(6):1289-1301.
15. National Cancer Institute Common Terminology Criteria for Adverse Events, version 4.0. 2009. (2016). https://evs.nci.nih.gov/ftp1/CTCAE/CTCAE_4.03/Archive/CTCAE_4.0_2009-05-29_QuickReference_8.5x11.pdf.
16. Witter AR, Okunnu BM, Berg RE. The essential role of neutrophils during infection with the intracellular bacterial pathogen listeria monocytogenes. *J Immunol*. 2016;197:1557-1565.
17. Hampton HR, Chtanova T. The lymph node neutrophil. *Semin Immunol*. 2016;28:129-136.
18. Baxter LT, Zhu H, Mackensen DG, Butler WF, Jain RK. Biodistribution of monoclonal antibodies: scale-up from mouse to human using a physiologically based pharmacokinetic model. *Cancer Res*. 1995;55:4611-4622.
19. Price PS, Conolly RB, Chaisson CF, et al. Modeling interindividual variation in physiological factors used in PBPK models of humans. *Crit Rev Toxicol*. 2003;33:469-503.
20. D'Argenio DZ, Schumitzky A, Wang X. *ADAPT 5 User's Guide: Pharmacokinetic/Pharmacodynamic Systems Analysis Software*. Los Angeles, CA: Biomedical Simulations Resource; 2009.
21. Smith CW. Transendothelial migration. In: Dunon D, Mackay CR, Imhof BA, eds. *Current Topics in Microbiology and Immunology*. Berlin, Heidelberg: Springer; 1993:201–212.
22. Tak T, Tesselaar K, Pillay J, Borghans JAM, Koenderman L. What's your age again? Determination of human neutrophil half-lives revisited. *J Leukoc Biol*. 2013;94:595-601.
23. Hsieh MM, Everhart JE, Byrd-Holt DD, Tisdale JF, Rodgers GP. Prevalence of neutropenia in the U.S. population: age, sex, smoking status, and ethnic differences. *Ann Intern Med*. 2007;146(7):486.
24. Athens JW, Raab SO, Haab OP, et al. Leukokinetic studies. III. The distribution of granulocytes in the blood of normal subjects. *J Clin Invest*. 1961;40(1):159-164.
25. Watari K, Asano S, Shirafuji N, et al. Serum granulocyte colony-stimulating factor levels in healthy volunteers and patients with various disorders as estimated by enzyme immunoassay. *Blood*. 1989;73(1):117-122.
26. Skubitz KM. Neutrophilic leukocytes. In: Greer JP, Arber DA, Glader B, List AF, Means RT, Paraskevas F, Rodgers GM, eds. *Wintrobe's Clinical Hematology*. 13th ed. Philadelphia: Welters Kluwer Lippincott Williams & Wilkins Health; 2014.
27. Zhu H, Melder RJ, Baxter LT, Jain RK. Physiologically based kinetic model of effector cell biodistribution in mammals: implications for adoptive immunotherapy. *Cancer Res*. 1996;56:3771-3781.
28. English D, Clanton JA. Evaluation of neutrophil labeling techniques using the chemotaxis radioassay. *J Nucl Med*. 1984;25:913-916.
29. Khot A, Matsueda S, Thomas VA, Koya RC, Shah DK. Measurement and quantitative characterization of whole-body pharmacokinetics of exogenously administered T cells in mice. *J Pharmacol Exp Ther*. 2019;368:503-513.
30. Zhang Y, D'Argenio DZ. Feedback control indirect response models. *J Pharmacokinet Pharmacodyn*. 2016;43:343-358.
31. Andrès E, Lorenzo Villalba N, Zulfiqar AA, Serraj K, Mourot-Cottet R, Gottenberg JE. State of art of idiosyncratic drug-induced neutropenia or agranulocytosis, with a focus on biotherapies. *J Clin Med.* 2019;8:1-18.
32. Akhtari M, Waller EK. Neutropenias in Felty's syndrome and systemic lupus erythematosus. In: Molineux G, Foote M, Arvedson T, eds. *Twenty Years G-CSF Clinical Nonclinical Discoveries*. Springer Basel; 2012:381-391.
33. Kelley WJ, Onyskiw PJ, Fromen CA, Eniola-Adefeso O. Model particulate drug carriers modulate leukocyte adhesion in human blood flows. *ACS Biomater Sci Eng*. 2019;5:6530-6540.
34. Harrold J, Gisleskog PO, Perez-Ruixo JJ, et al. Prediction of survival benefit of filgrastim in adult and pediatric patients with acute radiation syndrome. *Clin Transl Sci*. 2020;13:807-817.
35. Kovalenko P, Paccaly A, Boyapati A, et al. Population pharmacodynamic model of neutrophil margination and tolerance to describe effect of sarilumab on absolute neutrophil count in patients with rheumatoid arthritis. *CPT Pharmacometrics Syst Pharmacol*. 2020;9:405-414.

SUPPORTING INFORMATION

Additional supporting information may be found online in the Supporting Information section.

How to cite this article: Chen W, Boras B, Sung T, Hu W, Spilker ME, D'Argenio DZ. A whole-body circulatory neutrophil model with application to predicting clinical neutropenia from *in vitro* studies. *CPT Pharmacometrics Syst. Pharmacol.* 2021;10:671–683. https://doi.org/10.1002/psp4.12620